ACOUSTO-OPTIC INTERACTION

PACS numbers: 42.30.Lr; 42.79.Jq; 42.25.Fx
DOI: 10.1070/QE2010v040n09ABEH014371

Image transformation caused by wide-angle acousto-optic interaction

A.S. Machihin, V.E. Pozhar

***Abstract*. The problem of diffraction of divergent image-transfer light beams by an acoustic wave is considered. Expressions that describe the transfer function as a function of spectral and angular coordinates and are valid for any birefringence are obtained for the first time. The main characteristics of wide-angle acousto-optic tunable filters (angular and spectral bandwidths) are calculated and compared with the experimental data. The dependence of the transfer function on the angle of light incidence is investigated and a fundamental change in its topology is shown.**

Keywords: *acousto-optic tunable filter, birefringence, transfer function.*

1. Introduction

Spectral devices based on acousto-optic tunable filters (AOTFs) are widely used in various fields of research and technology [1 – 3]. Their advantages over devices using other physical principles are high throughput, high spatial and spectral resolution, and the possibility of modulating and synthesising the transfer function. In addition, random spectral access makes it possible to design spectral-adaptive systems based on AOTFs [4].

A key property of AOTFs is their ability to filter image-transfer beams, because these filters can be used for simultaneous analysis of the spatial and spectral properties of objects. As compared with other optical filters having this property, for example, liquid-crystal filters [2], AOTFs provide conversion in a wider spectral range (e.g., 0.4 – 0.8 μm) with a fairly high (for such compact devices) resolution (to 0.1 nm) [4, 5]. Although the diffraction is nonlocal (because occurs from bulk grating), AOTFs provide a satisfactory resolution (up to 1000 resolved points in each coordinate) and image quality.

To apply AOTFs in optical imaging systems, it is necessary to know how the image is transformed in diffracting light waves by a bulk diffraction grating formed by the acoustic wave. Effective diffraction is known to occur when the spatial matching condition for light and sound waves (Bragg condition) is satisfied. This condition has a simple geometric representation: the wave vectors of the incident ($\boldsymbol{k}_\mathrm{i}$) and diffracted ($\boldsymbol{k}_\mathrm{d}$) light waves and the acoustic

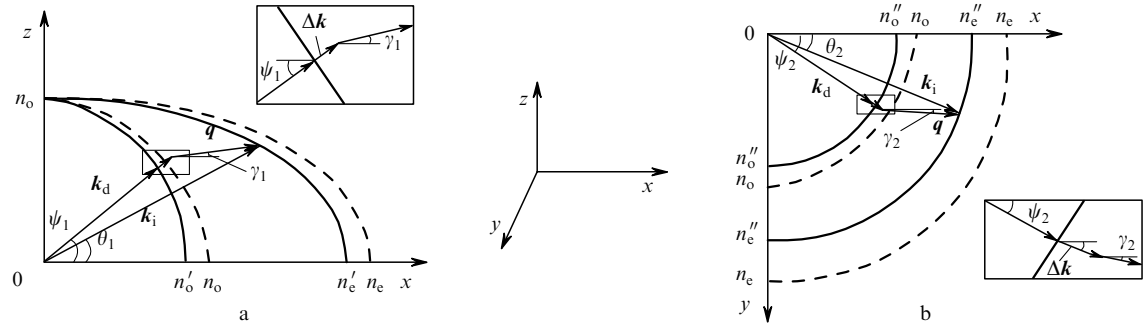

Figure 1. Wave diagram of AO interaction in the (a) polar and (b) azimuthal planes for anisotropic diffraction. ($\boldsymbol{k}_\mathrm{i}$, and $\boldsymbol{k}_\mathrm{d}$ are the wave vectors of the incident and diffracted light waves; $\boldsymbol{q}$ is the wave vector of the acoustic wave; $\Delta\boldsymbol{k} = \boldsymbol{k}_\mathrm{i} - \boldsymbol{q} - \boldsymbol{k}_\mathrm{d}$ is the wave mismatch (all angles are counted counterclockwise from the x axis); $k = 2\pi/\lambda$; n_o and n_e are, respectively, the refractive indices of ordinary and extraordinary polarised waves; γ_1 and γ_2 are the propagation angles of sound; and ψ_1 and ψ_2 are the propagation angles of diffracted wave.

A.S. Machihin, V.E. Pozhar Scientific and Technological Centre of Unique Instrumentation, Russian Academy of Sciences, ul. Butlerova 15, 117342 Moscow, Russia;
e-mail: aalexanderr@mail.ru, vpozhar@rambler.ru

Received 4 June 2010; revision received 2 July 2010
Kvantovaya Elektronika **40** (9) 837 – 841 (2010)
Translated by Yu.P. Sin'kov

wave ($\boldsymbol{q}$) should form a triangle (Fig. 1). Using this condition, one can relate the orientation $\boldsymbol{q}$ and frequency f of the acoustic wave and the propagation direction $\boldsymbol{k}_\mathrm{d}$ and wavelength λ_s of the effectively diffracted plane light wave; this relation is the basis of AO filtration. However, to calculate the characteristics of a real AOTF, which deals with divergent polychromatic light, it is necessary to describe the diffraction of light waves with other wave-

lengths ($\lambda = \lambda_s + \Delta\lambda$) and other propagation directions ($\theta_1 = \theta_{1s} + \Delta\theta_1$ and $\theta_2 = \theta_{2s} + \Delta\theta_2$). Hereinafter, λ_s, θ_{1s}, and θ_{2s} are, respectively, the wavelength and propagation angles of the incident light, which satisfy the matching condition for a specified sound wave $\boldsymbol{q}$.

The image transformation (Fig. 2) comprises spatial deformations, which describe the relative displacement of each image point, caused by the deflection of the corresponding plane light wave during diffraction, and the amplitude conversion. The latter is described by the intensity transfer coefficient, which is determined by the diffraction efficiency of the corresponding wave. The deformations and losses caused by other factors (along with the diffraction from acoustic wave) are disregarded here, because they can be taken into account by conventional optical methods. In monochromatic light spatial deformations comprise a linear image extension along the optical axis and nonlinear deformations (distortion) [6, 7]. When filtering white light, one should take into account chromatic aberrations: spectral shift, magnification chromatic aberration, etc. The purpose of this study was to analyse the amplitude distortions caused by acousto-optic (AO) diffraction; in particular, to calculate the angular and spectral dependences of the transfer coefficient $T(\theta_1, \theta_2, \lambda)$.

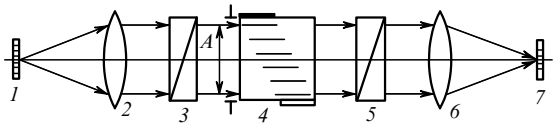

Figure 2. Schematic diagram of image transfer during AO filtration: (*1*) initial image (object); (*2*, *6*) objectives; (*3*, *5*) crossed polarisers; (*4*) AO cell; (*7*) spectral image; (*A*) entrance aperture of AOTF.

Until now, the characteristics of light diffraction from a sound wave were calculated either numerically for each individual configuration or using some approximations, which significantly facilitate analysis. In particular, the small birefringence approximation ($\Delta n/n \ll 1$) is used, which *a fortiori* reduces the estimation accuracy. In addition, the analysis is generally restricted to evaluation of the diffraction characteristics in the polar (symmetric) plane and perpendicularly oriented azimuthal plane (Fig. 1). The insufficiency of this approach follows even from the fact that in the general case of diffraction Bragg triangle belongs to none of these planes.

In this context, we stated, considered, and solved for the first time the problem of finding the transfer function $T(\theta_1, \theta_2, \lambda)$ corresponding to diffraction of divergent light beams by an ultrasonic wave at an arbitrary birefringence $\Delta n/n$ for arbitrary propagation directions of light and sound. The exact expressions obtained for the wave mismatch $\Delta\boldsymbol{k}$ are used to calculate the basic parameters of imaging AOTFs: spectral resolution and angular aperture. The calculated characteristics are compared with the known experimental data. A general analysis of the forms of transfer function is also performed and its radical transformation with a change in the angle of incidence is revealed. Possible practical applications of the results obtained are discussed.

2. Method

When solving the problem of describing the anisotropic light diffraction from sound in uniaxial crystals in the most general case (i.e., without the above-mentioned approximations), we first obtained the basic relations, linking the spectral and angular parameters, and then used these relations to derive in the general form all particular formulas that are necessary for further analysis. These formulas were checked by comparing with experimental data and by considering the limiting transition to the expressions known in the literature, which describe the diffraction in polar and azimuthal planes in the small-birefringence approximation.

Then we derived expressions for the spectral-angular dependence of the wave mismatch, which determines the form of the transmission function T of the AOTF in any specific geometry, from the basic relations, taking into account the corresponding particular formulas. The behaviour of this function was investigated at a continuous change in the angular variable, which describes the transition from one geometry to another, and revealed some features of the function transformation, which have not been described previously.

3. Basic relations

Using the Bragg triangle (Fig. 1), with the given propagation angles of sound (γ_1, γ_2) and light (θ_1, θ_2), one can determine in the general form the diffracted wave propagation direction $\boldsymbol{k}_d$ (i.e., the direction corresponding to the minimum wave mismatch Δk) for any sound wavelength Λ and light wavelength λ. The angles ψ_1 and ψ_2, corresponding to this direction, and the Δk values are given by the general expressions [6]

$$\psi_1 = \arctan\Big\{[\xi(\theta_1)\sin\theta_1 - \eta\sin\gamma_1]\big\{[\xi(\theta_1)\cos\theta_1 - \eta\cos\gamma_1]^2 + 2\eta\xi(\theta_1)\cos\theta_1\cos\gamma_1[1-\cos(\theta_2-\gamma_2)]\big\}^{-1/2}\Big\}, \quad (1a)$$

$$\psi_2 = \arctan\left[\frac{\xi(\theta_1)\cos\theta_1\sin\theta_2 - \eta\cos\gamma_1\sin\gamma_2}{\xi(\theta_1)\cos\theta_1\cos\theta_2 - \eta\cos\gamma_1\cos\gamma_2}\right], \quad (1b)$$

$$\Delta k = kn_o\Big\{\big\{[\xi(\theta_1)-\eta]^2 + 2\eta\xi(\theta_1)[1-\cos(\theta_1-\gamma_1) + \cos\theta_1\cos\gamma_1(1-\cos(\theta_2-\gamma_2))]\big\}^{1/2} - 1\Big\}. \quad (1c)$$

Here, $k = 2\pi/\lambda$; λ is the light wavelength in vacuum; $\eta = q/(kn_o) = \lambda/(\Lambda n_o)$ is the dimensionless spectral parameter, which determines the ratio of the light wavelength λ and sound wavelength Λ; $\xi(\theta_1) = n_e(\theta_1)/n_o = n_e(n_o^2\cos^2\theta_1 + n_e^2\sin^2\theta_1)^{-1/2}$ is the parameter characterising the birefringence; n_o and $n_e(\theta_1)$ are the refractive indices of the crystal material for ordinary and extraordinary polarised waves, respectively; $n_e = n_e(0)$. Note that the ξ value, as well as n_o and n_e, is spectrally dependent. The characteristics ψ_1, ψ_2, and Δk in formulas (1) are functions of six parameters: θ_1, θ_2, λ, Λ, γ_1, γ_2.

Since effective diffraction occurs only in the case of exact matching, Eqn (1c), under the condition $\Delta k = 0$, yields the dependence of the diffracted wave wavelength ($\lambda \propto \eta$) on the

orientation angles of the sound wave γ_1, γ_2 and the angles of incident light θ_1, θ_2:

$$\eta_s = \chi - \left[\chi^2 - \xi^2(\theta_1) + 1\right]^{1/2}, \tag{2}$$

where $\chi \equiv \xi(\theta_1)\{\cos(\theta_1-\gamma_1)+[\cos(\theta_2-\gamma_2)-1]\cos\theta_1\cos\gamma_1\}$. Formula (2) is in fact the tuning characteristic of the AOTF, which relates the ultrasonic frequency $f = n_o(\lambda)\eta_s(\lambda)v/\lambda$ with the wavelength λ of the selected spectral component. Here, v is the speed of sound and the function $\eta_s(\lambda)$ takes into account the dispersion of crystal refractive indices $n_{o,e}(\lambda)$ at the selected spectral component of light. This dependence can easily be measured. The general formula (2) in the particular case of diffraction in the polar plane ($\theta_2 = 0$, $\psi_2 = 0$) coincides with the corresponding expression from [8].

Substituting expressions (2) into formulas (1a) and (1b), one can find the propagation direction of the diffracted wave (ψ_{1s}, ψ_{2s}) as a function of the incident wave direction (θ_1, θ_2) at a fixed orientation of the ultrasonic wave (γ_1, γ_2) for the spectral component η_s, which obeys the exact matching conditions. This function (it is not written explicitly here) determines in the most general form the law of image distortion at diffraction [6, 7], i.e., expresses the output angles ψ_1, ψ_2 in terms of the input angles θ_1, θ_2. In this study formula (1c) was used to calculate the transfer function $T(\Delta\theta_1, \Delta\theta_2, \lambda)$ for the most frequently used AOTFs. Beforehand, it is necessary to obtain in the general form all the formulas describing the diffraction in these filters.

4. Wide-angle geometry AO interaction

Most applications of AOTFs require a large angular aperture, for example, to provide a large angular field (for image transfer) or a large aperture ratio (in spectrometry). The maximum aperture of the AOTF is obtained when the tangents to the wave vector surfaces are parallel (Fig. 3) [6–9]. This condition can be written as an exact relation, expressing the angle ψ_1 of diffracted wave propagation, for which the exact matching condition is satisfied, through the angle θ_1 of incident wave propagation. Note that, by imposing the condition of a large angular aperture, the diffraction direction ψ_{1w} depends on only one variable – the angle of incidence θ_{1w}:

$$\tan\psi_{1w} = \xi_0^2 \tan\theta_{1w}, \tag{3}$$

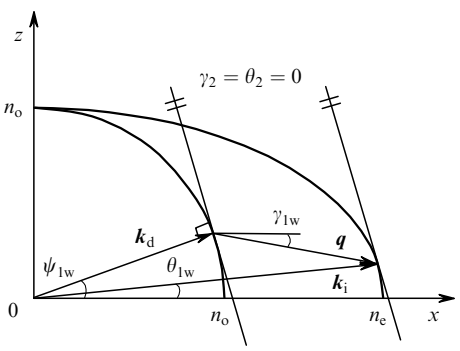

Figure 3. Wave diagram of wide-angle AO interaction in the polar plane.

where $\xi_0 = \xi(0) = n_e/n_o$; the subscript 'w' indicates the quantities corresponding to the wide-angle diffraction geometry.

In this case, the propagation angles of light (θ_{1w}) and sound (γ_{1w}) should be related as follows:

$$\tan\gamma_{1w} = -\frac{\xi_0 \tan\theta_{1w}}{\left[\left(\xi_0^4\tan^2\theta_{1w}+1\right)\left(\xi_0^2\tan^2\theta_{1w}+1\right)\right]^{1/2} + \xi_0^3\tan^2\theta_{1w}}. \tag{4}$$

Note also that formula (4), found from the geometric analysis of the Bragg triangle (Fig. 3), was obtained for the first time; it is valid for any birefringence. In the small-birefringence approximation ($\xi_0 \to 1$), which is generally used in calculations, the exact formula (4) takes a simple form:

$$\tan\gamma_{1w} = -\frac{\tan\theta_{1w}}{2\tan^2\theta_{1w}+1}, \tag{5}$$

which is identical to the expression $\tan(\theta_{1w} - \gamma_{1w}) = 2\tan\theta_{1w}$, derived in [7] in this approximation.

The relation between the angles θ_{1w} and γ_{1w} at wide-angle diffraction, which is described by (4), is a non-monotonic curve with a maximum, whose position and magnitude depend on the birefringence ξ_0 and, correspondingly, wavelength λ (Fig. 4).

The condition of parallelity of tangents (4) reflects the requirement for a maximally wide interval of wave matching, within which matching is retained at a deviation of the angle of incidence θ_1 from the optimal angle θ_{1w} (for a specified sound orientation γ_{1w}). The matching width increases even more near the maximum of $\gamma_{1w}(\theta_{1w})$, where the same angle θ_{1w} corresponds to a wide range of angles of incidence γ_{1w}. Therefore, this geometry is referred to as extreme [7] or optimal [9].

The angles θ_{ext} and γ_{ext}, which correspond to the extreme geometry of wide-aperture diffraction, were found from the exact formula (4) to be

$$\theta_{ext} = \operatorname{arccot}\left[\zeta^4\left(\zeta^2+1\right)^{1/2}\right],$$
$$\gamma_{ext} = -\operatorname{arccot}\left[\left(\zeta^2+1\right)^{3/2}\right], \tag{6}$$

where $\zeta = \xi_0^{1/3}$. The power 1/3 arises from the solution of the cubic equation when determining the extremum of $\gamma_{1w}(\theta_{1w})$. At a small birefringence ($\xi_0 \to 1$) these expressions yield the previously known values of the angles [7]:

$$\theta_{ext} \approx \arctan\left(\frac{1}{\sqrt{2}}\right) = 35.3^\circ,$$
$$\gamma_{ext} \approx -\arctan\left(\frac{1}{2\sqrt{2}}\right) = -19.5^\circ. \tag{7}$$

The exact expressions (6) for the extreme angles (derived for the first time) make it possible to calculate these angles for various materials and spectral ranges. For example, for paratellurite TeO_2 in the red spectral region (0.6 μm) a calculation yields $\gamma_{ext} = -18.9^\circ$ and $\theta_{ext} = 32.6^\circ$. These results coincide with the experimental data and previous estimates obtained by other methods [9].

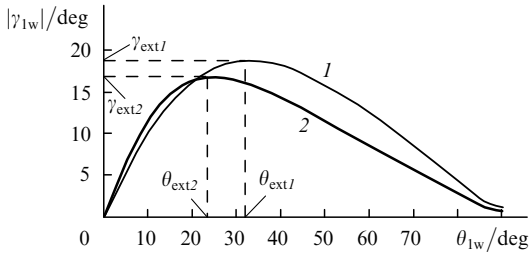

Figure 4. Necessary relationship between the angles of sound (γ_{1w}) and light (θ_{1w}) orientations at wide-angle diffraction for two materials: (*1*) TeO_2 ($\xi_0 = 1.07$, $\lambda = 0.6$ μm) and (*2*) Hg_2Cl_2 ($\xi_0 = 1.34$, $\lambda = 2$ μm).

Note that these values significantly differ from the limiting ones (7), despite the small birefringence in TeO_2 ($\xi_0 - 1 \approx 0.07$). As can be seen in Fig. 4, for calomel (Hg_2Cl_2), which has a much larger (but also small) birefringence ($\xi_0 - 1 \approx 0.34$), these differences are even more pronounced: $\gamma_{ext} = -16.9^\circ$ and $\theta_{ext} = 24.5^\circ$.

5. Collinear geometry

Axial collinear geometry is another geometry of AO interaction, which is often used in practice. In collinear filters the vectors of the ultrasonic wave ($\boldsymbol{q}$) and incident ($\boldsymbol{k}_i$) and diffracted ($\boldsymbol{k}_d$) light waves are collinear and directed along one of the crystal symmetry axes that are orthogonal to its optical axis, specifically: $\theta_1 = \theta_2$ and $\gamma_1 = \gamma_2 = 0$; thus, expressions (1) and (2) are simplified. This geometry, which is also wide-angle, provides a large wave interaction length, which is limited by only the sizes of the medium (crystal) L. As a result, one can obtain a higher spectral resolution ($\lambda/\Delta\lambda \propto L$) and reduce the control ultrasonic power ($P \propto L^{-2}$).

6. Transfer function

The transfer coefficient T related to AO diffraction is determined by the wave mismatch Δk. It is small when the sound power P is low: $T \sim (\Gamma L)^2 \mathrm{sinc}^2(\Delta k L/(2\pi))$, where $\mathrm{sinc}\, x \equiv [\sin(\pi x)]/(\pi x)$, wave coupling coefficient $\Gamma \propto \sqrt{P}$, and L is the AO interaction length [5]. With an increase in the sound power the transfer coefficient may reach 100 %. For example, in the case of plane wave diffraction (1D problem), the transfer coefficient is described by the formula

$$T = (\Gamma L)^2 \mathrm{sinc}^2 \left\{ \left[\Gamma^2 + \left(\frac{\Delta k}{2} \right)^2 \right]^{1/2} \frac{L}{\pi} \right\}; \qquad (8)$$

therefore, $T = 1$ in the case of exact matching ($\Delta k = 0$) and for a certain sound power ($\Gamma L = \pi/2$). It can be seen that in this case the transfer coefficient is also unambiguously related to the wave mismatch Δk. Hence, the above-stated problem of describing the angular and spectral dependences of the transfer coefficient $T(\theta_1, \theta_2, \lambda)$ is in fact reduced to determining the dependences of the wave mismatch Δk on the wavelength and propagation direction of the incident wave.

Assuming the sound propagation direction (γ_1, γ_2) to be fixed and the chosen sound frequency f_s to correspond to the light wavelength λ and direction (θ_1, θ_2) so that the Bragg condition is exactly satisfied, we will express the wave mismatch in terms of the angular coordinates $\Delta\theta_i = \theta_i - \Delta\theta_{is}$ (deviations from the match direction): $\Delta k(\Delta\theta_1, \Delta\theta_2, \lambda)$.

Substituting this expression into (8), we obtain the transfer function $T(\Delta\theta_1, \Delta\theta_2, \lambda)$, which demonstrates the nonuniformity of the transfer coefficient distribution over the image field. This function is described analytically based on the expressions obtained above and depends on the following parameters: interaction geometry, material of AOTF, ultrasonic power P, and interaction length L. Figure 5 shows the normalised transfer function $T(\Delta\theta_1, \Delta\theta_2)/(\Gamma L)^2$ for different geometries of wide-angle TeO_2 AOTFs ($\lambda = 0.6$ μm, $L = 1$ cm).

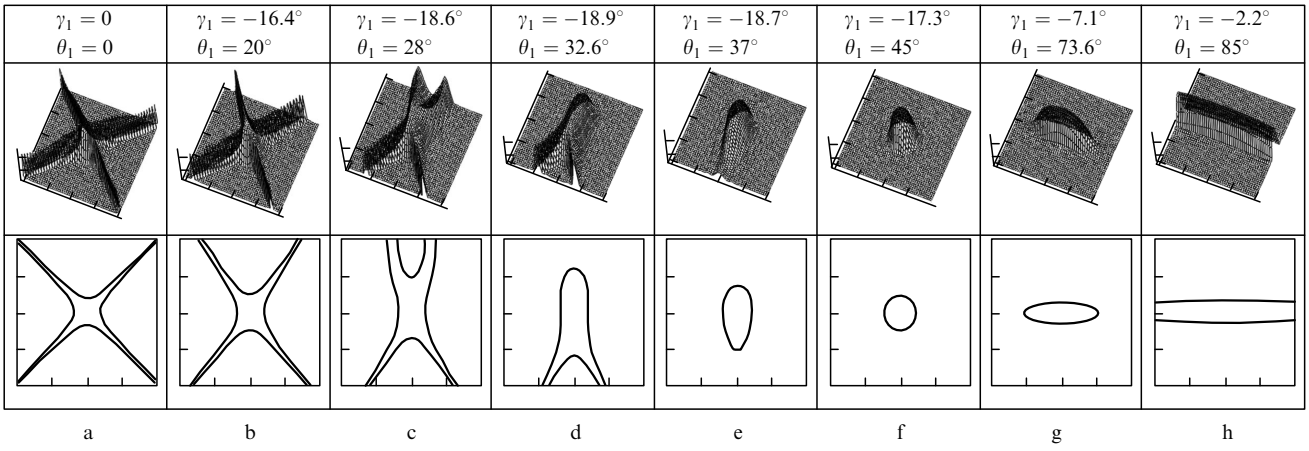

Figure 5. Normalised transfer function $T(\Delta\theta_1, \Delta\theta_2)/\Gamma^2 L^2$ of a wide-angle AOTF (top) and its cross section at a level of 0.5 (bottom); the range of angle variation along axes is from -5° to 5°.

It can be seen that the topology of this function depends strongly on the direction of light incidence θ_{1w} [and, correspondingly, the sound propagation angle $\gamma_{1w}(\theta_{1w})$], which is determined by the crystal 'cut-off angle'. In the range of small angles (near the axis) the cross section of the function is cross-shaped. Then, with an increase in θ_{1w}, the function is distorted and takes another form at $\theta_{1w} = \theta_{ext}$ (Fig. 5d). At $\theta_{1w} > \theta_{ext}$, with an increase in θ_{1w}, the cross section of the transfer function successively takes the forms of a vertical elongated closed area, a circle (at $\theta_{1w} \approx 45^\circ$), a

Table 1. Calculated and experimentally determined parameters of AOTFs.

Characteristics	Collinear axial AOTF (SiO_2)		Noncollinear wide-angle AOTF (TeO_2)	
	Calculation	Experiment	Calculation	Experiment
Angular aperture in crystal $(\delta\theta_1 \times \delta\theta_2)/\text{deg}$	2.2×2.2	2×2	1.7×6	$1.7 \times 1.7^*$
Angular aperture in air $(n_e\delta\theta_1 \times n_o\delta\theta_2)/\text{deg}$	3.4×3.4	3.1×3.1	4×14.4	$4 \times 4^*$
Number of resolved elements $(N_1 \times N_2)$	298×298	270×270	230×810	$250 \times 320^*$
Transmission window width $\delta\lambda/\text{nm}$	0.22	0.2	4	3.5
Spectral resolution $(R = \lambda/\delta\lambda)$	2900	3100	158	180

* The experiment was performed using a field diaphragm with a round hole, which limited the angular aperture of the AOTF in the azimuthal plane.

horizontal ellipse, and an area similar to a horizontal rectangular.

Thus, we analytically derived the transfer function of a wide-angle AOTF in the entire range of angle of light incidence (from 0 to 90°). Note that this function was numerically obtained in the form of a cross, circle, and elongated area in [10].

7. Calculation of parameters of AOTFs

Spectral resolution and angular aperture are the most important parameters of AOTFs. The spectral resolution $\lambda/\delta\lambda$ is determined by the width of the wavelength range $\delta\lambda$ within which effective light diffraction occurs. This range is found from the condition $|\Delta k(\Delta\lambda)| \leqslant \Delta k_{0.5} \approx \alpha L$, where the coefficient α takes values from 2.5 to 2.75 with a change in the diffraction efficiency from 0 to 100 % [5]. Similarly, the angular aperture $\delta\theta_1 \times \delta\theta_2$ of the AOTF is determined as the angular range, where $|\Delta k(\Delta\theta_1, \Delta\theta_2)| \leqslant \Delta k_{0.5}$. This value makes it possible to estimate the maximum number of image elements that can be resolved in both directions: $N_i = \delta\theta_i/\delta\theta_i^{\text{dif}}$, where $i = 1$, 2 and $\delta\theta_i^{\text{dif}} = 1.22\lambda/A_i$ is the diffraction divergence, which is determined by the sizes of the entrance aperture of the AOTF, A_i ($A_1 \times A_2$).

The formulas derived in this study make it possible to calculate the main characteristics of AOTFs. Table 1 contains the parameters calculated for two types of wide-angle AOTFs ($A_1 \times A_2 = 6 \times 6$ mm) that are used in practice [11, 12]: collinear axial filter (SiO_2, $\lambda = 0.633$ μm, $L = 18$ cm, $\xi = n_e/n_o = 1.006$, $\gamma_1 = 0$, $\theta_1 = 0$) and wide-angle filter (TeO_2, $\lambda = 0.633$ μm, $L = 1$ cm, $\xi = n_e/n_o = 1.067$, $\gamma_1 = -7.1°$, $\theta_1 = 73.6°$).

It can be seen that the calculated parameters are in good agreement with the experimental data. Note also that the angular aperture of a collinear AOTF is of the same size in both directions, whereas the angular aperture in an extreme wide-angle AOTF is significantly elongated in the polar plane (Fig. 5d).

8. Conclusions

We obtained the transfer function of AOTF, which describes the inhomogeneity of input image brightness. It allows one to determine the shape and sizes of the angular matching area, due to which the optimal angular aperture of AOTF can be chosen. The analysis performed revealed the dependence of the transfer function topology on the diffraction geometry. It was shown that, in contrast to collinear AOTFs, the aperture and spatial resolution of wide-angle filters significantly differ in the azimuthal and polar planes.

We derived expressions describing the relationship between the propagation angles of sound and incident and diffracted light, at which wide-angle diffraction is observed, including the general formulas for the angles θ_{ext} and γ_{ext} that describe the extreme geometry of wide-angle diffraction. These expressions are valid for crystals with arbitrary (in particular, large) birefringence ξ_0, for example, for calomel (Hg_2Cl_2) crystals ($\xi_0 = 1.34$). For clearness and uniformity, all figures and calculation examples are presented for only positive crystals (SiO_2, TeO_2, Hg_2Cl_2); nevertheless, the expressions derived are also valid for arbitrary uniaxial crystals.

The results of this study are important for designing wide-angle image-transfer AOTFs. They make it possible to calculate and analyse filter characteristics with a higher accuracy and take into account much more factors.

The approaches used here can be of interest for three-wave interaction problems, such as parametric light generation and generation of harmonics.

Acknowledgements. The study was performed on the basis of the Scientific and Educational Centre 'MATI-STC UI RAN' and supported by the Russian Foundation for Basic Research (Grant No. 09-02-12405). We are grateful to M.M. Mazur for helpful discussions and supplying experimental data.

References

1. Rajwa B., Ahmed W., Venkatapathi M., et al. *Proc. SPIE Int. Soc.Opt. Eng.*, **5694**, 16 (2005).
2. Morris H.R., Hoyt C.C., Treado P.J. *Appl. Spectr.*, **48** (7), 857 (1994).
3. Smith W.M.H., Smith K.M. *Experimental Astronomy*, **1** (5), 329 (1990).
4. Pozhar V.E., Pustovoit V.I. *Radiotekh. Elektron.*, **41** (10), 1272 (1996).
5. Anan'ev E.G., Pozhar V.E., Pustovoit V.I. *Opt. Spektrosk.* **62**, 159 (1987).
6. Machihin A.S., Pozhar V.E. *Zh. Tekh. Fiz.*, **80** (10), 101 (2010).
7. Pozhar V.E., Pustovoit V.I. *Photonics and Optoelectronics*, **4** (2), 67 (1997).
8. Voloshinov V. *Proc. SPIE Int. Opt. Eng.*, **3584**, 116 (1998).
9. Voloshinov V.B., Moskera Kh.S. *Opt. Spektrosk.*, **101** (4). 677 (2006).
10. Balakshii V.I., Kostyuk D.E. *Opt. Spektrosk.*, **101** (2). 298 (2006).
11. Anan'ev E.G., in *'Tochnye izmereniya v akustooptike i akustoelektronike'* (Precise Measurements in Acousto-optics and Acoustoelectronics) (Moscow: VNIIFTRI, 1985) p. 31.
12. Mazur M.M. *Doctoral Diss.* (Moscow: VNIIFTRI, 2007).